

A&A manuscript no.
(will be inserted by hand later)

Your thesaurus codes are:
11(02.12.2; 12.04.01; 11.09.4; 09.19.1; 13.19.1; 13.19.3)

ASTRONOMY
AND
ASTROPHYSICS
28.9.2018

Perspectives for detecting cold H₂ in outer galactic disks

Françoise Combes¹ and Daniel Pfenniger²

¹ DEMIRM, Observatoire de Paris, 61 Av. de l'Observatoire, 75 014 Paris, France

² Observatoire de Genève, CH-1290 Sauverny, Switzerland

Received ???; accepted ???

Abstract. We review here the main direct or indirect ways to detect the possible presence of large amounts of cold molecular hydrogen in the outer parts of disk galaxies, an hypothesis that we have recently developed. Direct ways range from H₂ absorption in the UV domain to detection of the radio hyperfine structure: the ortho-H₂ molecule has an hyperfine, or ultrafine, structure in its fundamental state, due to the coupling between the rotation-induced magnetic moment, and the nuclear spin. This gives rise to 2 magnetic dipole transitions, at the wavelengths of 0.5 and 5.5 km. Indirect ways are essentially the detection of the HD and LiH transitions, and in some environments like clusters of galaxies, more heavy trace molecules such as CO. We discuss from this point of view the recent discovery by COBE/FIRAS of a very cold Galactic dust component (4 – 7 K) which could correspond to a dominating gas mass component of the ISM, if interpreted as standard dust emission. Some of the proposed means could be applied to the well-known molecular clouds, to bring some new light to the problem of the H₂/CO conversion ratio.

Key words: line: identification – dark matter – galaxies: ISM – ISM: structure – radio lines: galaxies – radio lines: interstellar

1. Introduction

Molecular hydrogen has been recognized for a long time to be potentially the most important (baryonic) element in the Universe (Zwicky 1959), or at least in the Galaxy (Gould, Gold & Salpeter 1963) (see also the review by Field et al. 1966 and references therein). Since the late sixties the availability of millimetric radio-telescopes allowed to find substantial amounts of molecular hydrogen in locations where it can be traced by the CO molecule,

the molecular clouds. Roughly, the indirect detection of molecular hydrogen by the CO doubled the known gas content of spirals.

However, in metal poor regions where CO can hardly trace H₂, the question is still open. Most of the mass in the outer, metal poor parts of a galaxy could be very cold H₂, and remains invisible even today. The present trend to increase the conversion factor X between the CO intensity and the H₂ mass at decreasing metallicity goes in this direction (e.g. Sakamoto 1996).

The difficulty to detect the molecule H₂ comes from its symmetry, cancelling any electric dipole moment in the ground state. This prevents the detection of any radio line in emission, the only ones to be excited from the ground state in the cold interstellar medium ($T \approx 10$ K). The first H₂ lines to be detected in emission occur only by quadrupole radiation: they are the pure rotation ones, the first being the $J = 2 - 0$ at 28μ wavelength, already at 512 K above the fundamental state, the $J = 3 - 1$ at 17μ and $J = 4 - 2$ at 12μ (Beck et al. 1979, Parmar et al. 1994), and $J = 2 - 0$, and 2.12μ ($v = 1 - 0$, $J = 3 - 1$), corresponding to an excitation energy of ≈ 7000 K. These lines trace hot H₂ gas, for example excited in supersonic shocks, which corresponds to an insignificant fraction of the H₂ mass (e.g. Shull & Beckwith 1982). Many recent results obtained with the ISO satellite, with the SWS instrument sensitive between 2 and 45μ , have revealed the detection of more than a dozen of these ro-vibrational H₂ lines (Timmermann et al. 1996). These lines are emitted by very dense and warm gas ($T > 700$ K) in shocks, or even hot gas ($T \sim 11'000$ K), that is likely excited non-collisionally through UV pumping (Wright et al. 1996). In the violent starburst Arp 220, the H₂ emitting warm gas could represent up to 10% of the ISM mass (Sturm et al. 1996).

The only direct information on colder H₂ gas has been gained through far UV absorption in front of stars in the solar neighbourhood by the Copernicus satellite (e.g. Spitzer & Jenkins 1975). Unfortunately, only very diffuse clouds could be traced, since high H₂ column densities are associated with large extinctions. The density

(lower than 1 cm^{-3}), the molecular fraction (0.25) and temperature ($\approx 80 \text{ K}$) are typical of diffuse intercloud material. The dense and much colder molecular cloud bulk component remains to be explored.

In a recent model, we propose that the dark matter detected around spiral galaxies through flat rotation curves, is composed for a substantial part of cold molecular gas, in near isothermal equilibrium with the cosmic background temperature at 3 K (Pfenniger et al. 1994). This gas forms a hierarchical structure, possibly a fractal of dimension $D < 2$, spread over more than six orders of magnitude in scale ($\approx 100 \text{ pc}$ down to 10 AU). At the smaller scale, the tiniest fragments or “clumpuscles” are evolving in the adiabatic regime (Pfenniger & Combes 1994). They have an average density of $10^{9-10} \text{ cm}^{-3}$, a column density of $10^{24-25} \text{ cm}^{-2}$, and a Jupiter mass ($10^{-3} M_{\odot}$). Their surface filling factor is less than 1% (simply estimated by the ratio of the average Galactic and clumpuscle column densities). Due to the intrinsic inhomogeneity of the fractal structure, the collision time-scale of the clumpuscles and larger clumps is shorter than their collapse time.

So the envisaged equilibrium is dynamical, constantly renewed collisions in a slight supersonic regime prevent statistically most of the otherwise expected collapses that would lead to jupiter or star formation. Note that the collision speed at the bottom of the hierarchy is of the order of 0.2 km s^{-1} , so “shocks” do not imply necessarily strong heating in such conditions. The frequent collisions mean also that the average temperature and density of the clumpuscles are associated with large fluctuations, the warmer tail of the distribution being just the observed HI. Indeed collisions not only tend to heat by mechanical compression, they also simultaneously *cool* by gravitational coupling, an often overlooked effect due to the negative specific heat of gravitating systems. Of course in such a model a 100% inefficiency of jupiter or star formation can not be excluded. However we expect that for the same yet poorly understood reasons that prevent normal molecular clouds to form stars efficiently (as a naive expectation about collapsing gas would lead to believe), similar mechanisms must exist in low excitation regions such as outer galactic disks and Malin 1 type galaxies preventing the the fast cooling HI to collapse immediately.

This model explains naturally the evolution of galaxies along the Hubble sequence. Through gas accretion, the dark matter in the outer parts of late-type galaxies is progressively transformed into stars while galaxies evolve towards earlier types. It also explains the near constant surface density ratio between the HI gas and dark matter in the outer parts of spirals (Bosma 1981). During galaxy interactions, some of the cold gas of the outer parts is progressively heated, and accounts for the huge amounts of hot gas detected through X-ray emission in rich galaxy clusters.

With similar argumentation variant models have also been recently proposed, in which H₂ gas contributes signif-

icantly to the dark matter, based mainly in massive proto globular cluster clouds possibly mixed with brown dwarfs (de Paolis et al. 1995, Gerhard & Silk 1996). In this case, the cold H₂ gas is not *very* cold, but has a temperature between 5 and 20 K, which makes it easier to detect in emission. However, in the mixed model it is hard to see how any substantial fractions of cold gas and brown dwarfs can coexist without virializing rapidly the gas temperature to much higher values than 5 – 20 K, via dynamical friction and cluster core collapses.

If most of the mass of the Galaxy is under the form of molecular gas, are there more or less direct ways to detect it? In this article, we review several, some novel, possibilities, and try to select the most promising ones. To our knowledge a similar earlier attempt was made only in the 60’s (Gould & Harwit 1963), so the tremendous changes made in between justify a new article on the subject. We first describe the ultrafine structure of the ortho-H₂ in its ground state, due to the interaction between the nuclear spin ($I = 1$) and the magnetic moment induced by the nuclear rotation ($J = 1$), which splits the fundamental in three sublevels ($F = 0, 1$ and 2). Then we consider trace molecules, formed in the big-bang nucleosynthesis, HD, LiH, which could be seen in emission due to their electric dipole rotational transitions, or ions such as H₂⁺ that could be detected through its hyperfine structure. Also, traces of metal enrichment of this quasi-primordial gas could help to detect it through CO emission or absorption. Since very cold gas is more likely to be detected in absorption, we evaluate the probability to detect UV absorption lines of H₂ in front of remote quasars. Finally, we discuss the submillimeter continuum emission of very cold dust.

The possibility to trace cold gas through their interaction with cosmic rays and production of gamma rays will be discussed in a subsequent paper in which the highly inhomogeneous gas distribution of the ISM will be taken into account.

2. The hyperfine structure of the ortho-H₂

The hydrogen molecule can be found in two species, the para-H₂, in which the nuclear spins of the two protons are anti-aligned, and the resulting spin $I = 0$. Then, the spin wave function is anti-symmetric, and the nuclear wave function must be symmetric. Since the two electrons are paired in the molecule, their total spin and angular momentum is zero. The angular momentum of the molecule is then only due to the rotation. In the fundamental state $J = 0$, for which there is a symmetric wave-function.

For the ortho-H₂, on the contrary, the total nuclear spin is $I = 1$, since the spins of the two protons are parallel. The spin wave function being symmetrical, the nuclear radial wave function must be antisymmetric, by Pauli exclusion principle. Then, the fundamental state of ortho-H₂ is $J = 1$.

2.1. The energy split

The rotation of the molecule creates a rotational magnetic moment parallel and proportional to the angular momentum J , since charged particles (the protons) are in rotation. This rotational moment interacts with the nuclear spin I , through an interaction of the form $k\mathbf{I} \cdot \mathbf{J}$. In other words, this comes from the interaction of M_I , the nuclear spin magnetic dipole, with the magnetic field created from the motion of charges due to rotation. To this interaction, must be added the spin-spin magnetic interaction for the two nuclei, and the interaction of any nuclear electrical quadrupole moment with the variation of the molecular electric field in the vicinity of the nucleus (Kellogg et al. 1939, 1940; Ramsey 1952). In negligible external magnetic field, the H₂ states can be expressed by the reference basis of F, m_F , with $F = 0, 1, 2$. Magnetic dipole transitions are possible for $\Delta F = 1$, i.e., there are two transitions, $F = 2 - 1$, and $F = 1 - 0$. Measurements of these frequencies in the laboratory have been carried out through magnetic resonance on molecular beams (Kolsky et al. 1952; Harrick & Ramsey 1953). The wavelength of these two transitions have been measured at 0.5 and 5.5 km, or more precisely at frequencies of 546.390 kHz and 54.850 KHz respectively for $F = 1 - 0$ and $F = 2 - 1$.

The reason of such a low energy split of the hyperfine structure is due to the only interaction between nuclear momenta. When the fine structure is due to interaction between electronic momenta, the usual hyperfine structure corresponds to interaction between electronic and nuclear momenta. The fine structure splitting is then proportional to the Bohr magneton $\mu_o = eh/(4\pi m_e c)$ squared, where m_e is the electron mass. The hyperfine structure involves the product of μ_o with the nuclear magneton $\mu_n = eh/(4\pi m_p c)$, where m_p is the proton mass. When the interaction involves two nuclear momenta, the splitting is proportional to μ_n^2 , i.e. smaller than the hyperfine structure by roughly a factor m_p/m_e . This could be called ultrafine structure (cf. Field et al. 1966).

2.2. The ortho-para ratio

Only the ortho-H₂ is concerned by the ultrafine structure. Normal molecular hydrogen gas contains a mixture of the two varieties, with an ortho-to-para ratio of 3 when the temperature is high with respect to the energy difference of the two fundamental states (171 K). For instance, in the warm H₂ gas detected by ISO-SWS, an ortho-to-para ratio of 3 is compatible with observations (Wright et al. 1996). At lower temperatures, the ortho-to-para ratio must be lower, if the thermodynamical equilibrium can be reached, until all the hydrogen is in para state at $T = 0$. However, due to the rarefied density of the ISM, the ortho-to-para ratio is frozen to the H₂-formation value (Schaefer, private communication). Considerable densities are required for

the ortho-to-para conversion, which occurs in solid H₂ for instance.

But the fractal gas must be seen as a dynamical structure far out of thermodynamical equilibrium, not only with large density contrasts, but also large temperature contrasts, extending to low temperature the well know inhomogeneous properties of the ISM where it can be well observed, i.e. above about 10 K. The HI is then the warm interface, and H₂ the coldest component, in a mass ratio of about 1 to 10. By continuity, H₂ forms from HI and vice versa with a rate given by the clump collision time-scale at the scale corresponding to the virial temperature of the transition. This is in any case relatively short: at a scale corresponding to a temperature of 3000 K, and a fractal dimension $D \sim 1.7$, we estimate a duty-cycle time of transformation HI to H₂ of the order of 10^{6-7} yr, the cold and warmer phases must be chemically well mixed. This is an important difference with the alternative cold gas models of de Paolis et al. and Gerhard & Silk, were gas clumps, modeled as classical gas blobs, require stability over a substantial fraction of a Hubble time.

Now the key role in ortho to para conversion in interstellar clouds is the proton exchange reaction ($\text{H}^+ + \text{H}_2(j = 1) \rightarrow \text{H}^+ + \text{H}_2(j = 0)$), cf. Dalgarno et al. 1973; Gerlich 1990). This reaction can transform the ortho in a time-scale $5 \cdot 10^{13} n(\text{H}_2)^{-1/2}$ s, if the H^+ ions in dense clouds are essentially due to cosmic ray impacts, with the ionizing flux $\xi = 10^{-17} \text{ s}^{-1}$ characteristic of the solar neighbourhood. The corresponding time-scale for a clump near the Sun is 10 yr, and the ortho fraction is negligible, but at large distances in the Galaxy outskirts, where the cosmic-ray flux is expected to fall exponentially to zero, we can expect a significant part of ortho-H₂ in the cold gas.

3. Detectability of the H₂ ultrafine lines

On the Earth, the ionosphere is reflecting the long wavelength radiations, and this phenomenon is used for radio transmission all over the world (communications with submarines, for example, can be made through km wavelengths signals). The ionospheric plasma is filtering all frequencies below the plasma frequency $\omega = e(4\pi n/m_e)^{1/2} \approx 100$ MHz. It is therefore necessary to observe from space. Even from space, the long wavelength radiations are somewhat hindered by interplanetary or interstellar scintillations (e.g. Cordes et al. 1986). This means, as shown below, that spatial resolution above 1° could not be obtained below 0.1 MHz.

3.1. Interstellar plasma

The plasma frequency in the interstellar medium can be estimated by $\nu_p = 9 n_e^{1/2}$ kHz, where n_e is the electron density in cm^{-3} . Since the latter is in average of the order of 10^{-3} cm^{-3} , the plasma frequency $\nu_p \approx 250$ Hz. Radi-

ation of frequencies below that value does not propagate in the medium. More precisely, since the ISM is far from homogeneous, low-frequency radiation propagates in rarefied regions, and is reflected and absorbed by denser condensations. For the kilometric wavelengths that we are interested in, there is no problem of propagation, but the waves are scattered due to fluctuations in electron density. The electric vector undergoes phase fluctuations, since the index of refraction is $(1 - \nu_p^2/\nu^2)^{1/2}$, where ν is the radiation frequency. If the ISM is modeled by a Gaussian spatial distribution of turbulent clumps of size a , the scattering angle can be expressed by:

$$\theta_{\text{scat}} \approx 10^8 \left(\frac{L}{a}\right)^{1/2} \frac{\langle \Delta n_e^2 \rangle^{1/2}}{\nu^2} \text{ radian} \quad (1)$$

where L is the total path crossed by the radiation, and ν is the frequency in Hz (e.g. Lang 1980). At a typical distance of $L = 3$ kpc, and for the frequencies considered (≈ 200 kHz), the scattering angle is of the order of one degree. The scintillation problem is therefore severe, and hinders spatial resolution for point sources, but it is still possible to map the Galactic disk.

The interplanetary medium produces somewhat less scattering, and the total order of magnitude remains unchanged.

3.2. Intensity of the H₂ ultrafine lines

The radiation has a dipole matrix element proportional to μ_n^2 ; the line intensity is therefore much weaker than for usual hyperfine transitions (magnetic dipole in μ_o^2). Since the spontaneous emission coefficient A is proportional to ν^3 , the life-time of a hydrogen molecule in the upper ultrafine states is much larger than a Hubble time: $A \approx 10^{-32} \text{ s}^{-1}$. It is then likely that the desexcitation is mostly collisional. Even at the 3 K temperature, the upper levels are populated in the statistical weights ratio. A weak radiation is therefore expected, but the velocity-integrated emission ($\int T_a dv$) is ten orders of magnitude less than for the HI line, for the same column density of hydrogen. The prospects to detect the lines are scarce in the near future, since it would need an instrument of about 6 orders of magnitude increase in surface with respect to nowadays ground-base telescopes! A solution could be to dispose a grid of cables or array of dipoles spaced by $\lambda/4 \approx 125$ m on a significant surface of the Moon, e.g. an area of $(300 \text{ km})^2$. This requirement could be released, however, if there exists strong coherent continuum sources at km wavelengths. The H₂ ultrafine line could then be detected much more easily in absorption, with presently planned km instruments.

3.3. Galactic background and VLF projects

Several groups have studied the possibility to observe the sky in the very low frequency domain ($\approx 0.5 - 15$ MHz);

the most important projects being the NASA Low Frequency Space Array (LFSA) (Weiler et al. 1988, 1994), and ESA Very Low Frequency Array (VLFA, ESA Report, SCI96-002). These are space projects, since the Earth ionosphere is opaque below 15 MHz. The present projects now consider the possibility either of satellites orbiting the Moon, or an array of dipoles on the Moon itself, to avoid the strong radio interferences coming from the Earth. On the Moon, the hidden far-side surface is favoured, to be completely free of the Earth radio emissions. However, the lunar ionosphere might add some problems, especially on the lunar day, so the observations would be confined to the 14 days lunar night.

The limit at low frequency (0.5 MHz) is fixed by interstellar free-free absorption: the optical depth depends on the emission measure of the medium ($\int N_e^2 dx$) and its electron temperature (T_e). Typically, the depth l that we can see through the medium below $\tau = 1$ is a function of frequency ν in MHz: $l \sim (50\nu)^2 \text{ pc}$. At the lower frequency 0.5 MHz, the observations will just cross the Galactic plane, and be able to see extragalactic sources. One cannot rely on the clumpy structure of the medium to see through it (as for dust in the optical domain), since the scattering effects of the turbulent plasma broaden any emission to an angle $\theta \sim 22'\nu^{-2}$, i.e. $\sim 1.5^\circ$ at 0.5 MHz.

The sensitivity of such arrays depends only on their total surface and filling factor f , but not on the receivers quality, since the system temperature is dominated by the sky noise itself (galactic background radiation, essentially of synchrotron origin), which is about $3 \cdot 10^7 \text{ K}$ at 0.5 MHz. Arrays of short dipoles (10 m) on the Moon covering 100 km diameter surface are considered, with a filling factor of $f \sim 10^{-3}$. The signal to noise ratio reached in an integration time t in a frequency band $\Delta\nu$ is then $\text{SNR} = f\sqrt{(\Delta\nu t)}$, and can reach $\text{SNR} = 200$ in $t = 14$ days. In other words, we could detect signals at a few percent of the galactic background within a lunar night.

In front of such an intense Galactic background, the H₂ molecules are absorbing at their line frequency of 0.5 MHz. However the optical thickness could be at most $\tau = 10^{-5}$ in condensed regions, and smoothed to an average of $\tau = 10^{-10}$ in regions subtended by the effective resolution of $\sim 1.5^\circ$. Observations of an absorbing signal will only be possible towards very strong continuum sources such as Cas-A, and in any case will be quite difficult.

4. The HD and LiH Transitions and Detectability

HD has a weak electric dipole moment, since the proton in the molecule is more mobile than the deuteron; the electron then does not follow exactly the motion of the positive charge, producing a dipole. This moment has been measured in the ground vibrational state from the intensity of the pure rotational spectrum by Treffer & Gush (1968): its value is $5.85 \pm 0.17 \cdot 10^{-4}$ Debye. The first ro-

tational level is at ≈ 130 K above the ground level, the corresponding wavelength is 112μ . This line could be only observed in emission from heated regions, and given the very low abundance ratio $\text{HD}/\text{H}_2 \approx 10^{-5}$ and weak dipole, does not appear as a good tracer of the cold gas.

The LiH molecule has a much larger dipole moment, $\mu = 5.9$ Debye (Lawrence et al. 1963), and the first rotational level is only at ≈ 21 K above the ground level, the corresponding wavelength is 0.67 mm (Pearson & Gordy 1969; Rothstein 1969). The line frequencies in the sub-millimeter and far-infrared domain have been recently determined with high precision in the laboratory (Plummer et al. 1984, Bellini et al. 1994), and the great astrophysical interest of the LiH molecule has been emphasized (e.g. Puy et al. 1993). A tentative has even been carried out to detect LiH at very high redshifts (de Bernardis et al. 1993). This line is unfortunately not accessible from the ground at $z = 0$ due to H₂O atmospheric absorption. This has to wait the launching of a submillimeter satellite, but is a good candidate. The abundance of LiH has been recently estimated to a very low value ($< 10^{-15}$) in the post-recombination epoch (Stancil et al. 1996). The rate coefficient for LiH formation through radiative association is now estimated 3 orders of magnitude smaller than previously (Lepp & Schull 1984). In very dense clouds, however, three-body associations reactions have to be taken into account, and most of the lithium turns into molecules; an order of magnitude for LiH abundance is then $\text{LiH}/\text{H}_2 \approx 10^{-10}$, and the optical depth should reach 1 for a column density of 10^{12} cm^{-2} , or $\text{N}(\text{H}_2) = 10^{22} \text{ cm}^{-2}$, in channels of 1 km s^{-1} . The line should then be easily detectable in normal molecular clouds, within the optical disk of the Galaxy; the more so as the primordial abundance of Li could be increased by about a factor 10 in stellar nucleosynthesis (e.g. Reeves 1994). In the outer Galaxy parts of course, the same problems of excitation arise for a very cold gas, and the surface filling factor might be a problem for absorption measurements.

5. The H₂⁺ hyperfine transitions

The abundance of the H₂⁺ ion is predicted to be no more than 10^{-11} to 10^{-10} in chemical models (e.g. Viala 1986). But the H₂⁺ ion possesses an hyperfine structure in its ground state, unfortunately in the first rotational level $N = 1$. The electron spin is $1/2$, and the nuclear spin $I = 1$, which couple in $F_2 = I + S = 1/2$ and $3/2$; then $F = F_2 + N = 1/2, 3/2$ and $5/2$. Five transitions are therefore expected, of which the strongest is $F, F_2 = 5/2, 3/2 \rightarrow 3/2, 1/2$, at 1343 MHz (Sommerville 1965; Field et al. 1966). At the interface between the cold molecular gas and the interstellar/intergalactic radiation field, one can hope to encounter a sufficient column density of H₂⁺. The excitation to the $E_u = 110$ K level is problematic however.

6. C and O enrichment of the quasi-primordial gas

6.1. CO in emission or absorption

The usual tracer of molecular hydrogen in the ISM is the CO molecule, but is valid only for enriched gas, and fails at large distances from galaxy centers. The abundance $[\text{O}/\text{H}]$ decreases exponentially with radius in spiral galaxies, with a gradient between -0.05 and -0.1 dex/kpc (e.g. Pagel & Edmunds 1981), and the $\text{N}(\text{H}_2)/\text{I}(\text{CO})$ conversion ratio is consequently increasing exponentially with radius (Sakamoto 1996). There could be even more dramatic effects such as a sharp threshold in extinction (at 0.25 mag) before CO is detectable (Blitz et al. 1990), due to photodissociation. The effect of metallicity on the conversion ratio has long been debated (e.g. Elmegreen 1989), but strong evidence exists in the Magellanic Clouds (Rubio et al. 1993), and in nearby dwarf galaxies (Israel, Tacconi & Baas 1995; Verter & Hodge 1995; Wilson 1995). The fact that the CO line is optically thick does not make it insensitive to metallicity, since the observed size of molecular clouds is related to the $\tau = 1$ surface, and clouds appear much smaller at low metallicity. This fact is often ignored in theoretical models, where clouds or clumps are assumed to have a constant column density with radius (e.g. Wolfire et al. 1993).

It is easy to estimate until which radius the dense clouds are likely to contain CO molecules, if we estimate that the opacity gradient follows the metallicity gradient. Assuming the proportionality relation $\text{N}(\text{H}) \approx 2 \cdot 10^{21} A_v \text{ atoms cm}^{-2} \text{ mag}^{-1}$ between the gas column density and opacity in the solar neighbourhood (Savage et al. 1977), and a column density of 10^{25} cm^{-2} for the densest fragments, their opacity A_v falls to 0.25 at $R \approx 60$ kpc, but of course the CO disappears on large scales before.

Another effect hinders the detection of molecular tracers in emission, far from star-formation regions, which is the lack of heating sources. It is impossible to detect emission from a cloud at a temperature close to the background temperature. Only absorption is possible, although difficult for a surface filling factor of less than 1%. Absorption is biased towards diffuse clouds, or intercloud medium, which has a large filling factor, and a low density (and therefore a low excitation temperature). This is beautifully demonstrated in the molecular absorption survey of Lucas & Liszt (1994, 1996) in our Galaxy: practically all of the absorbing clouds are diffuse ($A_v \lesssim 1$) with a low excitation temperature. When the gas becomes metal deficient, the diffuse medium is preferentially depleted in molecules, through UV photo-dissociation.

6.2. Intracluster gas

It might still be possible in special environments such as galaxy clusters, to try to detect the cold gas, polluted by the enriched intra-cluster medium. The problem is to estimate the actual enrichment, based on the gas mixing. The

medium is expected to be multi-phase from theoretical calculations (e.g. Ferland et al. 1994), and direct EUVE observations of the $5 \cdot 10^5$ K gas in the Virgo cluster (Lieu et al. 1996) support a substantial cooling of the X-ray gas toward cold phases. In the outer parts of the cluster, before galaxy interactions have heated the cold gas around individual galaxies, the latter is still cold and metal deficient. Progressively the cold gas is heated and transferred in the hot X-ray emitting phase, where it is metal enriched, at least to the intra-cluster abundance of $\approx 0.3 Z_{\odot}$. In the cluster center, where the density of hot gas is high enough, the hot phase becomes unstable to cooling, and generates the cooling flow. Since there is no reason why the ubiquitous hierarchical fragmentation observed in the Galaxy is not universal, we must expect that in galaxy cluster gas fragmentation occurs too down to low temperature, small sizes and high densities, i.e. to molecular clumpules (Pfenniger & Combes 1994). This accounts for the apparent complete disappearance of gas in cooling flows, and may explain the high concentration of dark matter in clusters deduced from X-ray data and gravitational arcs (Durret et al. 1994; Wu & Hammer 1993).

Many authors have tried to detect this gas in emission or absorption, either in HI (Burns et al. 1981; Valentijn & Giovanelli 1982; Shostak et al. 1983; McNamara et al. 1990; Dwarakanath et al. 1995) or in the CO molecule (Grabelsky & Ulmer 1990; McNamara & Jaffe 1994; Antonucci & Barvainis 1994; Braine & Dupraz 1994; O’Dea et al. 1994). Maybe the best evidence of the presence of the cooling gas is the extended soft X-ray absorption (White et al. 1991). Although the HI is not detected in emission with upper limits of the order of $10^9 - 10^{10} M_{\odot}$, it is sometimes detected in absorption, when there is a strong continuum source in the central galaxy. The corresponding column densities are $> 10^{20} \text{ cm}^{-2}$. There is also some CO emission in Perseus A (Lazareff et al. 1989), but which may come from the galaxy itself and not the cooling flow.

To produce the X-ray absorption observed, the gas must have a high surface filling factor (≈ 1), and a column density of the order of $N_{\text{H}} \approx 10^{21} \text{ cm}^{-2}$ (White et al. 1991). The total mass derived is of the order of $10^{11} M_{\odot}$ over a 100 kpc region. This gas can only correspond to the atomic gas envelope of the denser, low filling factor, molecular clouds. If the molecular clouds are cold ($T \approx 3$ K) and condensed (filling factor $< 1\%$), it is extremely difficult to detect them, either in emission or in absorption, even at solar metallicity. The best upper limits reported in the literature ($N(\text{H}_2) < 10^{20} \text{ cm}^{-2}$, average over regions 10 kpc in size, but assuming $T \approx 20$ K and solar metallicity, i.e. the standard $N(\text{H}_2)/I(\text{CO})$ conversion ratio, are perfectly compatible with the existence of a huge cold H₂ mass (the conversion factor tends to infinity when the temperature tends to the background temperature). The HI gas, on the contrary, could give much significant constraints, since it is a warm gas with high filling factor. The column density detected in absorption are all compat-

ible to what is expected from the cooling flows. The HI gas is observed redshifted, falling on the central galaxy. Why is there no emission? It could be that the absorbing gas is too cold, and/or part of the gas absorbing X-rays is ionized (as observed H α filaments suggest).

That the molecular gas can cool down to ≈ 2.7 K within the intra-cluster environment has been demonstrated by Ferland et al. (1994), but debated (e.g. O’Dea et al. 1994). O’Dea et al. (1994) evaluate the X-ray heating rate of molecular clouds, assuming that the attenuating column density can be no more than 10^{21} cm^{-2} ($\tau = 0.2$ to 2) measured by White et al. (1991). But this assumes that the absorbing medium is homogeneous. On the contrary, if a hierarchical structure of dense molecular clouds is embedded within this HI envelope, the attenuating column density can be 3 or 4 orders of magnitude ($\tau \gg 1$) locally ($f < 1\%$); the molecular fragments can be completely screened from the X-ray flux. The presence of the X-ray flux introduces a warm ionized interface between the very cold molecular gas and the hot medium. That might be this phase that is seen in soft X-ray absorption by White et al. (1991). The HI absorption measurements reveal that only a small part of this interface is neutral.

Recently, Lieu et al (1996) and Bowyer et al (1966) have detected large quantities of gas at intermediate temperature of $5 \cdot 10^5$ K in the Virgo and Coma clusters with the EUVE satellite (Extreme UltraViolet Explorer). Since this gas is cooling very rapidly, being near the peak of the radiative cooling curve, it should be very transient. Although its extension coincides with that of the cooling flow, the mass flow involved would be 30 times that of the cooling flow itself. Its detection is therefore not only evidence for a continuous flow of gas cooling from the high virial temperature of the clusters (10^7 K), but also of possible other heating mechanisms like shocks. Also the detection of the near-infrared quadrupolar emission line H₂(1-0)S(1) in central cluster galaxies with cooling flows (and their non-detection in similar control galaxies without cooling flows) strongly confirms the gas flow as it passes through the temperature of 2000K (Jaffe & Bremer 1997).

7. H₂ absorption lines in front of quasars

Absorption should be the best way to trace the cold gas. If the effective gas temperature is indeed close to the background T_{bg} , emission is extremely weak. The antenna temperature is, in the Rayleigh-Jeans approximation:

$$T_{\text{a}} = (T_{\text{ex}} - T_{\text{bg}}) (1 - e^{-\tau}) \quad (2)$$

where T_{ex} is the gas excitation temperature and τ the optical thickness in the transition considered. On the contrary, absorption is biased towards cold gas, since the observed signal is proportional to N_0/T_{ex} , where N_0 is the column density in the ground state.

7.1. Detected H₂ absorption lines

Absorption in the vibration-rotation part of the spectrum (in infrared) is not the best method, since the transitions are quadrupolar and very weak. An H₂ absorption in Orion has been detected only recently (Lacy et al. 1994) and the apparent optical depth is only about 1%. This needs exceptionally strong continuum sources, which are rare. Electronic lines in the UV should be more easy to see in absorption.

However, recognizing molecular hydrogen absorption in UV spectra of quasars is not easy due to the dense Ly α forest. Many tentatives have remained inconclusive. A careful cross-correlation analysis of the spectrum is needed in order to extract the H₂ lines from the confusion. Already Levshakov & Varshalovich (1985) had made a tentative detection, towards PKS 0528–250, with some 13 coincident lines among the Lyman and Werner H₂ bands. But molecular hydrogen has been firmly found in absorption in front of the quasars PKS 0528–250 (Foltz et al. 1988) and QSO 0013–004 (Ge & Bechtold 1997). These objects are at redshifts $z = 2.8$ and $z = 1.97$ respectively and are viewed through damped Ly α systems; the inferred H₂ column densities are 10^{18} cm⁻² and $7 \cdot 10^{19}$ cm⁻², with estimated widths of 5 and 15 km s⁻¹ and kinetic temperatures of 100 and 70 K. These conditions, together with the molecular fraction derived $f_{\text{H}_2} = 0.002$ and 0.22, indicate a diffuse medium.

It should be remarked that only the very low column densities of H₂ can be detected this way, since for moderate to high molecular column densities, the line damping is so high that the quasar is no longer visible, as is developed in next paragraph. This happens in only rare cases, since the filling factor of high H₂ surface density gas is lower than $f = 1\%$. Unfortunately, it is not presently possible to observe H₂ absorptions at $z = 0$ from our own Galaxy in front of quasars, since the HST has no instrument at the right frequency (wavelengths smaller or equal to 1100 Å). The probability to have an intervening high molecular column density is of course very small at non-zero redshift. Moreover, for redshift high enough, the size of a dense clump is not large enough to cover the quasar UV continuum, and the depth of the absorption is not larger than $f = 1\%$. The possibility to detect H₂ absorption from our own Galaxy has to await future UV satellites, such as the Lyman-FUSE (Far-Ultraviolet Spectrographic Explorer) mission.

7.2. Line damping

For a high column density of H₂, such as 10^{25} cm⁻² as should be the case at the center of a clumpuscule, the absorption lines in the UV range is extremely saturated. In these circumstances, the actual width of the lines exceeds considerably the Doppler width, to be entirely dominated by the natural width. Radiation damping determines the

profile. While the Doppler width should be of the order of 0.1 km s⁻¹, the equivalent width must be computed from the “square-root” region of the curve of growth. The expected equivalent width W normalised to the wavelength λ can be crudely estimated to be $W/\lambda \sim 1$. This means that all H₂ lines in the Lyman and Werner bands are overlapping, and all the UV and optical light are absorbed. A special computation of the line profile should then been done, since the simple Lorentzian profile is no-longer valid far away from the resonance line (when $\Delta\nu \sim \nu$).

We have derived the total cross section of the interaction photon-molecule, including absorption and scattering. It can be shown (see Appendix) that this total cross-section, from the fundamental state, and in the vicinity of electronic dipolar transitions, can be written as:

$$\sigma(\omega) = \frac{\omega}{\epsilon_0 c \hbar} \sum_i |d_{0i}|^2 \frac{\left(\frac{\omega}{\omega_{0i}}\right)^3 \frac{\Gamma_i}{2}}{(\omega - \omega_{0i})^2 + \left(\frac{\Gamma_i}{2}\right)^2} \quad (3)$$

where the resonances occur for $\omega = \omega_{0i}$ (with corresponding dipole matrix element d_{0i}), and Γ_i is the natural width of the i -level. At low frequencies, the classical Rayleigh scattering formula in ω^4 is retrieved.

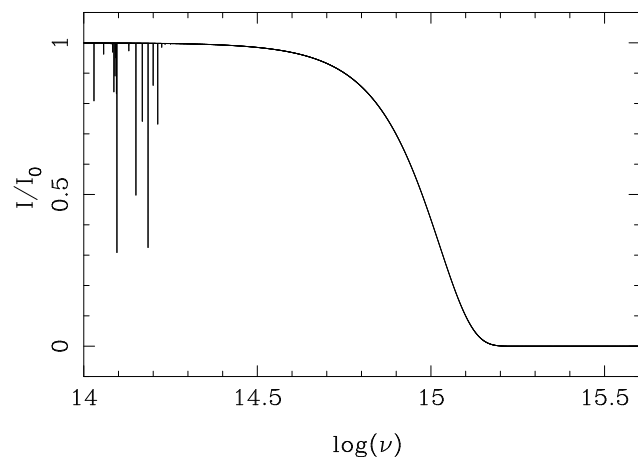


Fig. 1. Simulation of the absorption profile expected from a clumpuscule in the Milky Way in front of a remote UV quasar. Plotted is the ratio I/I_0 of the depth of the absorption normalised to the continuum. All the H₂ UV lines and NIR lines have been taken into account. The continuum has completely disappeared at high frequencies (λ smaller than 3000 Å, for a non-redshifted quasar).

This cross section has been taken into account to compute the expected profile in front of a clumpuscule (Fig. 1). At high frequency, the asymptotic limit of the total cross-section is the Thomson cross-section $\sigma_T = 6.6 \cdot 10^{-25}$ cm⁻². The high frequency wing of the H₂ lines is

then always optically thick. The clumpuscule is absorbing all light with wavelength smaller than the optical band.

Within this band, the H₂ clumpuscules play then the role of dusty globules, removing the whole continuum of the region (even the He lines could not be seen). Since their surface coverage is not large, however, they do not completely obscure the quasar source, depending on its size, but only a few percents of it. The type of absorption depends strongly on the relative distances. If the absorbing clouds belong to an intervening galaxy at high redshift ($z \geq 0.5$), the angular size of the obscuring clumpuscules is less than a micro-second, and the effect on the remote quasar would remain un-noticed. If the absorption comes from our own Galaxy, the angular size can be a fraction of an arcsecond, and the optical QSO could be entirely covered and obscured. Through proper motions of the absorbing globules, at about 100 km s^{-1} , this absorption can appear or disappear on scales of one year.

7.3. Helium lines

The most abundant primordial element after hydrogen is helium, which remains atomic in dense molecular clouds. We have not considered it as a good tracer candidate: only the UV lines could be detected in absorption, the first one being at 584 \AA . The intensities of the lines are similar to that of molecular hydrogen, the problems of line damping and of filling factors are comparable. The direct H₂ lines are therefore a better candidate. When the latter are damped, the He lines are also obscured. Only in the case of complete condensation of the H₂ molecules into ice, does the He lines become useful. Helium is then the most abundant gas, its pressure supporting the clumpuscule against a free-fall gravitational collapse.

8. Submillimeter Continuum

The far-infrared and submillimeter continuum spectrum from 100μ to 2 mm has been derived from COBE/FIRAS observations by Wright et al. (1991) and Reach et al. (1995). They show that in addition to the predominant warm dust emission, fitted by a temperature ranging from $T \approx 16$ to 21 K , according to longitude, there is evidence for a very cold component, with temperatures between $T = 4$ and 7 K , ubiquitous in the Galaxy, and somewhat spatially correlated with the warm component. The opacity of the cold component, if interpreted by the same dust emissivity model (varying with frequency as ν^2 , is about 7 times that of the warm component. Most of the gas mass would then be contained in this component, which is, relatively to the warm component, stronger at high latitude and away from the galactic center. This is clearly seen in the longitude dependence of the cold/warm power ratio, which shows a characteristic minimum towards zero longitude (Reach et al. 1995).

8.1. H₂ dimers

Schaefer (1996) proposes that the cold dust component detected by COBE/FIRAS might be due in fact to molecular hydrogen emission, as collision-induced dipole transitions: in small very high density fluctuations (at a fraction of “amagat”, i.e. a density of $4 \cdot 10^{18} \text{ cm}^{-3}$), the H₂ gas can emit a continuum radiation, corresponding to free-bound or free-free transitions of weakly and temporarily bound H₂ molecules, the dimers, and containing a large fraction of ortho-H₂. By symmetry the para-para complexes do not produce such a radiation. A good fit is found for the COBE spectra if the dense H₂ clouds follow the HI distribution in the outer parts of the Galaxy. At least this shows that a cold component (“dust”) is indeed associated to the warmer HI.

This weak-dipole radiation due to H₂ collisional complexes is an interesting possibility to detect the presence of cold molecular hydrogen. This kind of radiation has been identified in planetary atmospheres during the Voyager IRIS mission (Hanel et al. 1979). Only exceptionally dense regions could explain the signal detected by COBE, since the emission is proportional to the square of the density (Schaefer 1994). The required density then imposes the temperature ($T > 11 \text{ K}$), to avoid the transition to solid molecular hydrogen. Already we had remarked that at the present cosmic background temperature of $T_{\text{bg0}} = 2.726 \pm 0.01 \text{ K}$, the average pressure in the H₂ clumpuscules was about 100 times the pressure of saturated vapour, and that probably a small fraction of the molecular mass might be in solid form (Pfenniger & Combes 1994, and several references therein about previous papers discussing the possibility of hiding molecular hydrogen in solid form). Snow flakes of H₂ can improve the coupling with the CBR, but the large latent heat of 110 K per H₂ molecule and the lack of nucleation sites in metal poor gas may prevent a large mass fraction to freeze out. The condition of dimerization is then largely satisfied in the physical conditions of the clumpuscules ($T \approx 3 \text{ K}$, $n \approx 10^{10} \text{ cm}^{-3}$), and we expect continuum radiation to be emitted and absorbed by the H₂ collisional complexes, through collision-induced dipole moment. The absorption coefficient peaks in the submillimeter domain ($\lambda = 0.5 \text{ mm}$). The optical depth of each clumpuscule is however quite low, $\tau \approx 10^{-9}$. This radiation is not detectable, but for the densest fluctuations, where the density exceeds 1 amagat = $4 \cdot 10^{18} \text{ cm}^{-3}$. The total mass required in these fluctuations is already a few $10^7 M_{\odot}$ for the whole Galaxy. The rather steep dependence on density of the H₂ emission coefficient prevents the obtaining of a less crude model, the more so as the optical depth of the dust components are not yet exactly known.

8.2. Cosmic infrared background

Reach et al. (1995) have neglected any cosmic infrared background (CIBR) in their modeling, but it has been claimed by Franceschini et al. (1994) that 5 to 25% of the sky brightness in the submillimeter and far-infrared bands is in fact the CIBR coming from the integrated light of galaxies. In their model, early-type galaxies at high redshift are highly obscured, and most of their light coming from the intense star-formation phase is re-radiated in the FIR. The COBE data allows a significant fraction of the sky brightness for the CIBR, since there is some freedom in the relative contributions of the Galaxy and the isotropic backgrounds. In any case, however, the hypothesis of the existence of a CIBR does not solve the cold component problem. Reach et al. (1995) have tried, prior to their analysis, to subtract a CIBR component as high as that computed by Franceschini et al. (1994), but this did not change their conclusions about the existence of the two components, which temperatures were unaffected.

The basic problem in deriving the exact amount of the CIBR contribution is the subtraction of the foreground emission. Another recent interpretation of the COBE/FIRAS data has been put forward by Puget et al. (1996) and Boulanger et al. (1996). Their approach consists in modeling the foreground dust emission according to the Dwingeloo recent HI survey (cf. Hartmann 1994). They use the fact that the relation between the integrated HI emission and the far-infrared emission is almost linear, at least for weak HI emission, corresponding to column densities $N(\text{HI}) < 4 \cdot 10^{20} \text{ cm}^{-2}$. They consider only the high latitudes: $|b| > 30^\circ$, where the temperature of the dust can be fitted with a constant temperature $T = 17.5 \text{ K}$, with an emissivity varying as ν^2 . After subtracting this component, with the proportionality factor found between HI and FIRAS emission they also subtract the infrared emission associated with the ionized gas, equivalent to an average column density of $0.4 \cdot 10^{20} \text{ H cm}^{-2}$, (following a cosecant law variation with latitude). This is necessary, since there is a bias in the HI-FIR emission relation, i.e., some far-infrared emission exists at zero HI emission, and this is interpreted as coming from dust associated to ionized gas, not correlated with HI. The residual has then the spectrum of a very cold dust component, peaking around 250μ . However this treatment neglects completely the molecular contribution, which in our Galaxy is of the same order of magnitude in mass as the HI component. The H₂ component distribution cannot be accurately known, since the CO molecule is not a good tracer. It was claimed by Puget et al. (1996) that they avoid molecular hydrogen by selecting only low column density of HI ($< 4.5 \cdot 10^{20} \text{ cm}^{-2}$). However they have first smoothed out the HI map at the FIRAS resolution of 7° . The molecular component being very clumpy, its signature is completely washed out in the process. A typical high latitude cloud (HLC) detected in molecular transitions is in

average of 1 deg^2 extent (Magnani et al. 1996), so that its average HI column density of 10^{21} cm^{-2} becomes negligible, diluted by a factor 49. The average surface density of HLC's has been estimated by Magnani et al. (1996) already below the HI threshold of $4.5 \cdot 10^{20} \text{ cm}^{-2}$. This means that it is impossible to avoid molecular hydrogen at the FIRAS resolution.

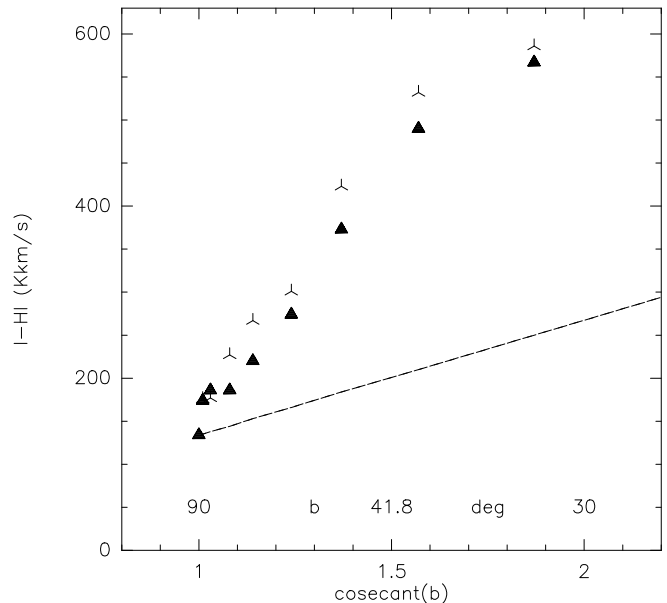


Fig. 2. Distribution of the HI emission with latitude in the Galaxy. The data come from the Bell-Labs survey (Stark et al. 1992). The crosses correspond to negative latitudes, and the filled triangles to positive b . The dashed line indicates the expected cosecant law, if the local HI plane could be approximated by a plane-parallel component.

8.3. Uncertainties in deriving the CIBR level

It is quite difficult to subtract local material emission from a possible isotropic component, since the distribution of the local material departs significantly from a plane-parallel geometry. It has been known from the first HI surveys that the Sun lies in a hole of HI deficiency (e.g. Burton 1976). The total column density of HI observed at the pole is $2 \cdot 10^{20} \text{ cm}^{-2}$, while it should have been twice higher through extrapolation of the $|b| = 30 - 40^\circ$ data. It is well known from many gas tracers that the Sun appears not too far from the center of an elongated Local Bubble mostly filled with hot gas, deficient in neutral gas, and of radius about $60 - 100 \text{ pc}$ (Welsh et al. 1994), approximately bounding the local ISM (LISM) (Cox & Reynolds 1987). The high latitude clouds observed in molecular transitions might be at the boundary of this cavity; their distribution does not show any longitude dependency, while it is also quite deficient at high latitude

(e.g. Magnani et al. 1996). The latitude distributions of the HI and IRAS 100 μ emission component depart from the expected cosecant law (e.g. Boulanger & Perault 1988, and Fig. 2), which might be attributed to the continuation of the Local Bubble in a high latitude chimney.

Note that between $|b| = 30$ to 90° , the region sampled is only the close neighbourhood of the Sun, within 500 pc or 1 kpc, according to the scale height of the medium (the HI scale height is 180 pc, and the H₂ 60 pc). Therefore, no longitude dependence is expected for $|b| > 15^\circ$.

If the neutral warm gas cannot be considered to follow the plane parallel geometry locally, i.e. there is a deficiency of warm dust associated to the HI gas at high latitude, this deficiency could be compensated by a colder medium, emitting only at the lower FIRAS frequencies. Indeed, the long wavelength (200 – 500 μ) emission from COBE/FIRAS does not suffer from this depletion, and follows better the cosecant law.

The correlation between the HI flux and the COBE/FIRAS emissions at wavelengths between 100 μ and 1 mm is in fact non-linear, as found by Boulanger et al. (1996). Also there appears to be some FIR-submm emission even at zero HI flux, which could be due to other gas components. It is therefore quite difficult to subtract the emission associated to the HI, since the results depend on the linear fit used, i.e. on the maximum $W(\text{HI})$ chosen. Boulanger et al. (1996) choose a rather low HI column density ($W(\text{HI}) = 250 \text{ K km s}^{-1}$), which induces strong selection effects as a function of latitude; indeed when averaged over longitude, the threshold $W = 250 \text{ K km s}^{-1}$ (or $N(\text{HI}) = 4.5 \cdot 10^{20} \text{ cm}^{-2}$) corresponds to $|b| > 42^\circ$. This range of latitude is not sufficient to reveal a cosecant law, since low column density regions at lower latitudes is not completely sampled (only the very low column densities are selected at lower latitudes).

Moreover, the mere subtraction of a linear FIR/HI fit, which underestimates the FIR at high latitude (low column density) and overestimates at low latitude (high column density) is able to create an isotropic residual.

The residual found by Puget et al. is comparable to the FIR flux at zero HI obtained through linear fitting of the FIR/HI correlations by Boulanger et al. (1996). This residual corresponds to FIR emission not associated to HI, and could come from colder gas than the HI (for example molecular). That would explain why its spectrum is shifted to long wavelengths. At least part of this residual could come from cold H₂ at high latitudes, that has not been properly sampled by CO.

The relative contributions of all these components are summarised in Fig. 3, where we have plotted as a function of longitude the flux of the cold and warm component at $b = 0^\circ$, as derived by Reach et al. (1995). When the fluxes of the various components are plotted as a function of latitude (Fig. 4), it can be noted that the cold component contribution appears indeed almost isotropic at $|b| > 50^\circ$. The cold component is also relatively more important out-

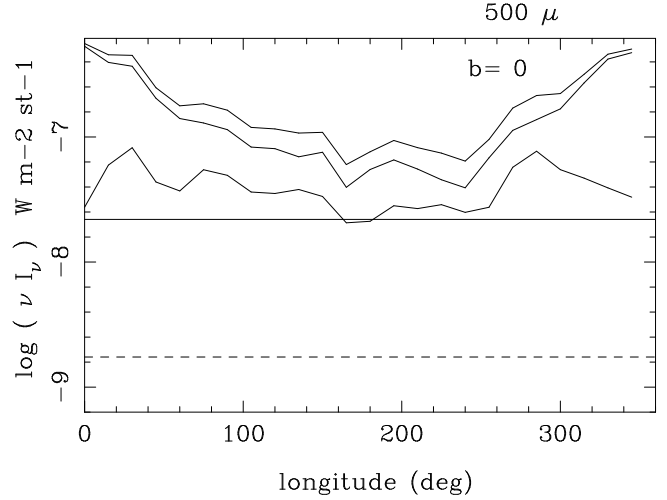


Fig. 3. Relative contribution at $\lambda = 500 \mu$ of the various components: the three broken lines correspond to the cold component (bottom), warm component (middle) and both together (top) analysed by Reach et al. (1995). The dashed horizontal line is the infrared isotropic background tentatively identified by Puget et al. (1996), and the full horizontal line is the CMBR component. At lower frequencies, λ between 500 and 1000 μ both the cold component and the CMBR increase relatively to the others.

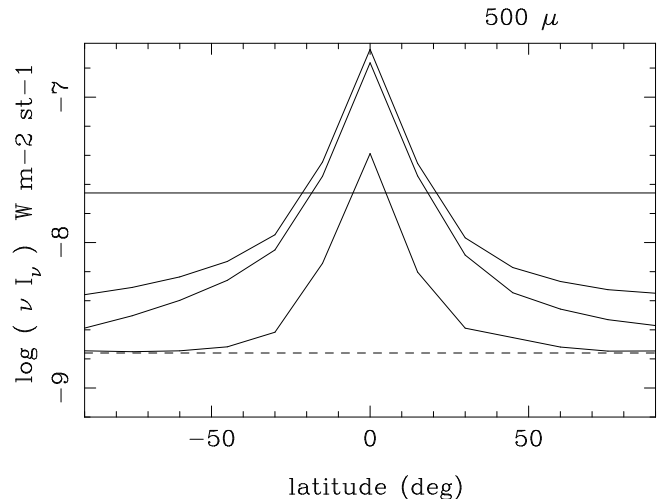


Fig. 4. Same as Fig. 3, but for the latitude dependence. The cold component appears relatively isotropic at $|b| > 50^\circ$. Note that the coincidence with the proposed level for the CIBR occurs only at 500 μ , since the spectra of the two components are different.

side of the Galactic center. Its longitude distribution corresponds to what is expected from a ring-like distribution, with a hole in the Galactic center.

It is important to note (cf. Fig. 3) that at $b = 0^\circ$, the cold component found by Reach et al. (1995) is 50 times higher than the CIBR, tentatively detected by Puget et al. (1996). This is obtained at $\lambda = 500 \mu$, but the ratio is even higher at lower frequencies (up to 100 at 1000μ), since the cold component has a lower temperature. The existence of the very cold component is inescapable. It cannot disappear, even in varying extensively the power α of the emissivity law.

9. Cold dust associated to dense cores in Giant Molecular Clouds

One of the best interpretation of the COBE-cold component could be dust associated to cold molecular hydrogen deep inside Giant Molecular Clouds (GMC), shielded from the ISRF by the high opacity of the cloud envelopes. That such cold component should exist is no surprise. It was already predicted by Mathis et al. (1983) in their investigation of the dust emission spectrum in both the diffuse ISM and in GMC's. From the determination of the dust absorption cross-section from the Lyman continuum to the submm range, and a model of the ISRF, they determine the radiation field inside a GMC, as a function of the optical depth from the surface. Assuming a typical homogeneous cloud, they find that the ISRF is absorbed in a very thin outer layer of the cloud. Inside the cloud the ISRF is converted entirely into FIR radiation, and its mean intensity is about five times the Galactic FIR emission. Only the thin outer layer of the clouds is heated enough to radiates at $60 - 100 \mu$: it corresponds to the warm dust traced by IRAS observations. It is well known that this dust mass represents only about 10% of the total dust mass (e.g. Thronson & Telesco 1986, Devereux & Young 1990). Well inside the GMC's, both silicate and graphite grains reach a temperature between 5 to 7 K (Mathis et al. 1983). This estimation did not include the clumping of gas, which could be responsible to even larger opacities, and lower grain temperatures.

If the existence of this cold gas could have been easily foreseen, the corresponding amount of gas was completely unknown. This is due to the fact that the molecular transitions are no longer a good tracer of H₂ mass at high density and low temperatures, as shown by studies of nearby molecular clouds, such as Orion. Of course, the main isotopic lines such as CO and CS are highly optically thick in such conditions, but also the rare isotopes, such as C¹⁸O or C³⁴S, are not good tracers of molecular condensations, certainly because of depletion of molecules on grains at high density (chemistry is not responsible, since the CO molecule is not destroyed at high density).

Mezger et al. (1992) and Launhardt et al. (1996) have mapped in the millimetric dust emission dense cores in the

Orion molecular cloud. They discover a certain number of condensations, where the dust emission peaks, which correspond to minima in dust temperature. The dust condensations *are not* or only barely visible in isotopic CO and CS transitions, probably because molecules have frozen out on dust grains (Mezger et al. 1992): it appears that molecule depletion becomes important at densities $n_H > 10^6 \text{ cm}^{-3}$, at least at low dust temperatures $T_d < 20 \text{ K}$. If the 1.3 mm emission of dust is a good pointer towards the dense cold condensations of the Orion GMC, they might not indicate the actual H₂ mass, because of large uncertainties in the physics of grains and their true opacities, and also in the actual temperature (they are determined around 15 K from the emission ratio between 870 and 1300μ). Virial masses determined from the CS line-widths are found 20 – 30 times higher than the gas mass derived from the 1.3 mm dust emission (Launhardt et al. 1996).

The mass in dense cold condensations can therefore only be traced by dust emission at long wavelength, such as with the COBE/FIRAS instrument (from 4.5 mm to 104μ). Although Reach et al. (1995) have discovered precisely such a cold component (4 – 7 K), they do not attribute it to cold dust, because it is also present at high latitude. Their argument is that these cold condensations must then be seen in the extinction maps at high latitude, and also their surface should be 100μ emitters in IRAS maps, and they are not observed. But these clouds are actually detected, both in the IRAS maps, and in extinction maps, and correspond to the well-known high latitude molecular clouds (HLC, Magnani et al. 1985). The surface filling factor of these HLC's has been debated. Magnani et al. (1986) estimated a surface filling factor of $5 \cdot 10^{-3}$, while Heithausen et al. (1993) find more than an order of magnitude larger, 13%, in mapping 620 deg^2 in the CO line with the CfA 1.2 m telescope. They find that the molecular surface density of these high latitude cirrus, projected on the Galactic plane, is between $N_H = 0.5 \text{ to } 1 \cdot 10^{20} \text{ cm}^{-2}$, which corresponds to 20% to 50% of the total molecular surface density of the Milky Way. However, the controversy is not so large when the limiting surface density is considered: Heithausen et al. (1993) find a larger surface filling factor, but they include larger and less opaque cloud envelopes. Magnani et al. (1996) in compiling all literature data confirm their filling fraction of $5 \cdot 10^{-3}$, which corresponds to 10–20% of the local Milky Way molecular surface density. The two estimations differ by a factor 2, and if we take the overlapping value of 20%, we end up with an average column density of $\langle N_H \rangle = 0.5 \cdot 10^{20} \text{ cm}^{-2}$. This estimation has been made with a low conversion factor for the HLC's: $N(\text{H}_2)/I(\text{CO})$ ratio of $0.5 \cdot 10^{20} \text{ mol cm}^{-2} \text{ K}^{-1} \text{ km}^{-1} \text{ s}$ for Heithausen et al. (1993), and a mixed range of values in the compilation of Magnani et al. (1996); this estimation is therefore highly uncertain (by up to an order of magnitude), and is likely to be a lower limit. The low conversion factor adopted for HLC's makes their mass much lower than the virial mass, and their CO abundance much

larger than that of local dark clouds (e.g. Boden & Heithausen 1993). The standard conversion ratio (cf. Strong et al. 1988) would lead to $\langle N_{\text{H}}(\text{HLC}) \rangle = 2.5 \cdot 10^{20} \text{ cm}^{-2}$. The value derived by Reach et al. (1995) for the cold component at high latitude ($|b| > 30^\circ$) corresponds to an average column density of $\langle N_{\text{H}} \rangle = 5 \cdot 10^{20} \text{ cm}^{-2}$, and is therefore compatible with the HLC value, within the uncertainties. Moreover, since Reach et al. have ignored any CIBR background, their average column density of the cold molecular material at high latitude could be somewhat overestimated (see Fig. 4). This overestimation of dust optical depth at high latitudes is acknowledged by Reach et al. (1995): they subtracted from the FIRAS spectra the brightest CIBR model from Franceschini et al. (1994), before repeating their spectral fit; the optical depths decreased, but the notable point is that the temperatures of the warm and cold components are barely affected.

Note that the remarkable correlation between optical depths of the cold and warm COBE components, even at high latitude, supports the interpretation of the cold component as coming from the cold dust shielded by the warm envelopes of the same clouds. The mean ratio 7 of optical depths found by Reach et al. (1995) reveals that the molecular mass of the Galaxy could be 7 times larger than previously assumed.

Whatever the origin of the cold component is, it might be a serious problem for measurements of cosmic microwave background fluctuations; it is not perfectly correlated spatially with the warm dust, and has the temperature and spectrum of the cosmological signal. Moreover, since it is likely that this component exists also in every spiral galaxy similar to the Milky Way, at a temperature $T_{\text{bg0}}(1+z)$, the integrated redshifted signals over all galaxies contribute also to the microwave fluctuations.

10. Conclusions

It is well established from the big-bang nucleosynthesis and observed abundances of primordial elements that the visible baryons today represent only a small fraction of all baryons that must exist in the Universe (cf. recent measurements by Tytler et al. 1996). The recent micro-lensing experiments conducted towards the Magellanic Clouds have revealed that Machos can account for 20% of this dark baryons (Aubourg et al. 1993; Alcock et al. 1996); the constraints are however weak and inconclusive because 0% as well as 100% are still values within the range allowed by the limited statistics of events and a robust estimate of all the errors involved.

Cold molecular hydrogen is one of the most appealing candidate (Pfenniger et al. 1994). Present observational constraints, when properly assessed, do not rule out this hypothesis. So we must search for observational tests to constrain or infirm the proposition.

The main difficulty to detect the cold gas in emission is its low temperature, close to the cosmic background temperature. The detection of the “ultrafine” structure of the ortho-H₂ molecules at km wavelengths raises considerable difficulties in the near future, but could be eventually a good means to fix the $N(\text{H}_2)/I(\text{CO})$ conversion ratio in our Galaxy. The HD and LiH rotational lines are or will be detectable by far-infrared satellites (ISO, FIRST, . . .), but their excitation energy is too high to trace the bulk of the cold gas. They could at best trace a perturbed fraction of it. In the same vein, the hyperfine structure line of H₂⁺ could be observed easily from the ground.

Absorption lines detection might be the best way if the gas is indeed very cold. Since the surface filling factor of the molecular clumps is low ($f < 1\%$), large statistics are required, but the perspectives are far from hopeless. H₂ absorption in the Lyman and Werner bands has already been identified in two damped Ly α systems. For a clumpuscule falling just on the line of sight of a quasar, we expect a damped absorption. It is then impossible to detect the quasar in the optical or UV, but in the near-infrared. Tracer molecules like CO in absorption are much less promising due to the low metallicity in addition to the low filling factor.

Finally, it is not excluded that the cold dust component detected by COBE/FIRAS (Reach et al. 1995) is tracing the cold H₂ component, limited to Galactic radii where the cold gas is still mixed with some dust. This cold component would be already 7 times more massive than the usual warm dusty ISM. As predicted by Mathis et al. (1983), the dense H₂ cores of Giant Molecular Clouds, shielded from the ISRF by large opacities, should keep an equilibrium temperature between 5 and 7 K. The fact that this cold medium is still observed at high latitude is not in contradiction with observations of high-latitude molecular clouds, given the large uncertainties in their true H₂ column densities. At high latitude, there could be also a contribution of the cosmic infrared background radiation; the latter is however negligible in front of the cold component at low latitude.

Acknowledgements. We are grateful to Claude Cohen-Tannoudji for enlightening discussions about the quantum mechanical treatment of photon-atom interactions, to Joachim Schaefer for interesting discussions about the H₂ molecule and its dimers, and to Dick Tipping for advice about far-wing profiles of molecular lines. This work was supported by the Swiss “Fond National de la Recherche Scientifique”.

References

- Abgrall H., Roueff E.: 1989, *A&AS* 79, 313
 Alcock C.A. et al.: 1996, *ApJ* 461, 84
 Antonucci R., Barvainis R.: 1994, *AJ* 107, 448
 Arnous E., Heitler W.: 1953, *Proc. Roy. Soc. A*, 220, 290
 Aubourg E. et al.: 1993, *Nature* 365, 623
 Bazell D., Désert F.X., 1988, *ApJ* 333, 353
 Beck S.C., Lacy J.H., Geballe T.R.: 1979, *ApJ* 234, L213
 Bellini M., de Natale P., Inguccio M., et al.: 1994, *ApJ* 424, 507
 Binney J., Tremaine S., 1987, *Galactic Dynamics*, Princeton Univ. Press, Princeton
 Blitz L., Bazell D., Désert F.X.: 1990, *ApJ* 352, L13
 Boden K-P., Heithausen A.: 1993, *A&A* 268, 255
 Bosma A.: 1981, *AJ* 86, 1825
 Boulanger F., Abergel A., Bernard J-P. et al.: 1996, *A&A* 312, 256
 Boulanger F., Péroul M.: 1988, *ApJ* 330, 964
 Bowyer S., Lampton M., Lieu R.: 1996, *Science* 274, 1338
 Braine J., Dupraz C.: 1994, *A&A* 283, 407
 Burns J.O., White R.A., Haynes M.P.: 1981, *AJ* 86, 1120
 Burton W.B. 1992, in: *The Galactic Interstellar Medium*, Saas-Fee Advanced Course 21, D. Pfenniger, P. Bartholdi (eds.), Springer-Verlag, Berlin, p. 1
 Burton W.B.: 1976, *ARAA* 14, 275
 Casertano S., van Albada T.J., 1990, in: *Baryonic Dark Matter*, D. Lynden-Bell, G. Gilmore (eds.), Kluwer, Dordrecht, p. 159
 Cohen-Tannoudji C., Dupont-Roc J., Grynberg G.: 1988, “Processus d’Interaction entre Atomes et Photons”, ed. Savoirs Actuels, CNRS-Intereditions
 Cordes J.M., Pidworbetsky A., Lovelace R.V.E.: 1986, *ApJ* 310, 737
 Cox D.P., Reynolds R.J.: 1987, *ARAA* 25, 303
 Dalgarno A., Black J.H., Weisheit J.C.: 1973, *Ap. Letters*, 14, 77
 de Bernardis P., Dubrovich V., Encrenaz P. et al.: 1993, *A&A* 269, 1
 de Paolis F., Ingrassio G., Jetzer Ph., Roncadelli M.: 1995, *A&A* 295, 567
 Devereux A.N., Young J.S.: 1990, *ApJ* 359, 42
 Diamond P.J., et al., 1989, *ApJ* 347, 302
 Dickman R.L., Snell R.L., Schloerb F.P.: 1986, *ApJ* 309, 326
 Durret F., Gerbal D., Lachièze-Rey M., Lima-Neto G., Sadat R.: 1994, *A&A* 287, 733
 Dwarakanath K.S., Owen F.N., van Gorkom J.H.: 1995, *ApJ* 442, L1
 Elmegreen B.G.: 1989, *ApJ* 338, 178
 Ferland G.J., Fabian A.C., Johnstone R.M.: 1994, *MNRAS* 266, 399
 Fiedler R.L., Dennison B., Johnston K.J., Hewish A., 1987, *Nat* 326, 675
 Field G.B., Somerville W.B., Dressler K.: 1966, *ARAA* 4, 207
 Foltz C.B., Chaffee F.H., Black J.H.: 1988, *ApJ* 324, 267
 Franceschini A., Mazzei P., De Zotti G., Danese L.: 1994, *ApJ* 427, 140
 Ge J., Bechtold J.: 1997, *ApJ* 477, L73
 Gerhard O., Silk J.: 1996, *ApJ* 472, 34
 Gerlich D.: 1990, *J. Chem. Phys.* 92, 2377
 Gould R.J., Gold T., Salpeter E.E.: 1963, *ApJ* 138, 408
 Gould R.J., Harwit M. 1963, *ApJ* 137, 694
 Grabelsky D.A., Ulmer M.P.: 1990, *ApJ* 355, 401
 Haiman Z., Rees M.J., Loeb A.: 1996, *ApJ* 467, 522
 Hanel R., Conrath B., Flasar M. et al.: 1979, *Science* 204, 972
 Harrick N.J., Barnes R.G., Bray P.J., Ramsey N.F.: 1953, *Phys. Rev.* 90, 260
 Hartmann D.: 1994, PhD thesis, University of Leiden
 Heithausen A., Stacy J.G., de Vries H.W., Mebold U., Thaddeus P.: 1993, *ApJ* 268, 265
 Israel F.P., Tacconi L.J., Baas F. 1995, *A&A* 295, 599
 Jaffe W., Bremer M.N. 1997: *MNRAS* 284, L1
 Kellogg J.M.B., Rabi I.I., Ramsey N.F., Zacharias J.R.: 1939, *Phys. Rev.* 56, 728
 Kellogg J.M.B., Rabi I.I., Ramsey N.F., Zacharias J.R.: 1940, *Phys. Rev.* 57, 677
 Kolsky H.G., Phipps T.E., Ramsey N.F., Silsbee H.B.: 1952, *Phys. Rev.* 87, 395
 Lacy J.H., Knacke R., Geballe T.R., Tokunaga A.T.: 1994, *ApJ* 428, L69
 Landau L., Lifchitz E.: 1989, “Physique théorique, Tome 4. Electrodynamique quantique”, Editions MIR, p. 300
 Lang K.R.: 1980, in *Astrophysical Formulae*, Springer-Verlag
 Larson R.B., 1992, *MNRAS* 256, 641
 Launhardt R., Mezger P.G., Haslam C.G.T. et al.: 1996, *A&A* 312, 569
 Lawrence T.R., Anderson C.H., Ramsey N.F.: 1963, *Phys. Rev.* 130, 1865
 Lazareff B., Castets A., Kim D.W., Jura M.: 1989, *ApJ* 335, L13
 Lepp S., Shull J.M.: 1983, *ApJ* 270, 578
 Levshakov S.A., Varshalovich D.A.: 1985, *MNRAS* 212, 517
 Lieu R., Mittaz J.P.D., Bowyer S., et al. 1996, *ApJ* 458, L5
 Lucas R., Liszt H.S.: 1994, *A&A* 282, L5
 Lucas R., Liszt H.S.: 1996, *A&A* 307, 237
 Magnani L., Blitz L., Mundy L., 1985, *ApJ* 295, 402
 Magnani L., Blitz L., Mundy L.: 1985, *ApJ* 295, 402
 Magnani L., Hartman D., Speck B.G.: 1996, *ApJS* 106, 447
 Magnani L., Lada E.A., Blitz L.: 1986, *ApJ* 301, 395
 Mathis J.S., Mezger P.G., Panagia N.: 1983, *A&A* 128, 212
 Mauersberger R., Wilson T.L., Mezger P.G., Gaume R., Johnston K.J.: 1992, *A&A* 256, 640
 McNamara B.R., Bregman J.N., O’Connell R.W.: 1990, *ApJ* 360, 20
 McNamara B.R., Jaffe W.: 1994, *A&A* 281, 673
 Mezger P.G., Sievers A.W., Haslam C.G.T. et al.: 1992, *A&A* 256, 631
 Mezger P.G., Wink J.E., Zylka R.: 1990, *A&A* 228, 95
 O’Dea C.P., Baum S.A., Maloney P.M., et al.: 1994, *ApJ* 422, 467
 Pagel B.E.J., Edmunds M.G.: 1981 *ARAA* 19, 77
 Parmar P.S., Lacy J.H., Achtermann J.M.: 1994, *ApJ* 430, 786
 Pearson E.F., Gordy W.: 1969, *Phys. Rev.* 177, 59
 Penprase B.E.: 1993 *ApJS* 88, 433
 Pfenniger D., Combes F., 1994, *A&A*, 285, 94
 Pfenniger D., Combes F., Martinet L., 1994, *A&A*, 285, 79
 Plummer G.M., Herbst E., de Lucia F.C.: 1984, *J. Chem. Phys.* 81, 4893
 Power E.A., Zienau S.: 1959, *Phil. Trans. Roy. Soc.* 251, 427
 Puget J-L., Abergel A., Bernard J-P., et al.: 1996, *A&A* 308, L5

- Puy D., Alecian G., Le Boulrot J., Léorat J., Pineau des Forêts G., 1993, *A&A* 267, 337
- Ramsey N.F.: 1952, *Phys. Rev.* 85, 60
- Reach W.T., Dwek E., Fixsen D.J. et al.: 1995, *ApJ* 451, 188
- Reach W.T., Pound M.W., Wilner D.J., Lee Y.: 1995, *ApJ* 441, 224
- Reeves H.: 1994, *Rev. Mod. Phys.* 66, 193
- Rothstein E.: 1969, *J. Chem. Phys.* 50, 1899 (Err. 52, 2804)
- Rubio M., Lequeux J., Boulanger F.: 1993, *A&A* 271, 9
- Sakamoto S. 1996 *ApJ* 462, 215
- Savage B.D., Bohlin R.C., Drake J.F., Budich W.: 1977, *ApJ* 216, 291
- Schaefer J.: 1994, *A&A* 284, 1015
- Schaefer J.: 1996, *Europhys. Lett.*, 34, 69
- Shostak G.S., van Gorkom J.H., Ekers R.D. et al.: 1983, *A&A* 119, L3
- Shull J.M., Beckwith S.: 1982, *ARAA* 20, 163
- Sodroski T.J., Odegard N., Arendt R.G. et al.: 1997, *ApJ* in press
- Sommerville W.B.: 1965, *J. Chem. Phys.* 43, 3398
- Spitzer L., Jenkins E.B.: 1975, *ARAA* 13, 133
- Stancil P.C., Lepp S., Dalgarno A.: 1996, *ApJ* 458, 401
- Stark A.A., Gammie C.F., Wilson R.W. et al.: 1992, *ApJS* 79, 77
- Strong A.W., Bloemen J.B.G.M., Dame T.M. et al.: 1988 *A&A* 207, 1
- Sturm E., Lutz D., Genzel R. et al.: 1996, *A&A* preprint
- Thronson, H.A., Telesco, C.M. 1986, *ApJ* 311, 98
- Timmermann R., Bertoldi F., Wright C.M. et al.: 1996, *A&A* 315, L281
- Trefler M., Gush H.P.: 1968, *Phys. Rev. Let.* 20, 703
- Tytler D., Fan X-M., Burles S.: 1996, *Nature* 381, 207
- Valentijn E.A., Giovanelli R.: 1982, *A&A* 114, 208
- Verter F., Hodge P. 1995, *ApJ* 446, 616
- Viala Y.P.: 1986, *A&AS* 64, 391
- Weiler K.W. et al.: 1994, NASA report
- Weiler K.W., Dennison B.K., Johnston K.J. et al.: 1988, *A&A* 195, 372
- Weisskopf V., Wigner E.: 1930, *Z. Phys.* 63, 54
- Welsh B.Y., Craig N., Vedder P.W., Vallerga J.V.: 1994, *ApJ* 437, 638
- White D.A., Fabian A.C., Johnstone R.M. et al.: 1991, *MNRAS* 252, 72
- Wilson C.D. 1995, *ApJ* 448, L97
- Wolfire M.G., Hollenbach D., Tielens A.G.G.M.: 1993, *ApJ* 402, 195
- Wright C.M., Drapatz S., Timmermann R. et al.: 1996, *A&A* preprint
- Wright E.L., Mather J.C., Bennett C.L. et al.: 1991 *ApJ* 381, 200
- Wu X.P., Hammer F.: 1993, *MNRAS* 262, 187
- Zwicky F. 1959: *PASP* 71, 468

A. Appendix

In this appendix, we compute the total cross section of the interaction between photons and cold molecular hydrogen, including absorption and scattering.

When a discrete excited level j is coupled to a continuum of states, the evolution of the system becomes ir-

reversible. This is the case for the spontaneous emission, where the probability to stay in the excited level decreases exponentially with time, $\propto e^{-\Gamma_j t}$. This defines a half-life $\tau = 1/\Gamma_j$, where Γ_j is the transition probability per unit time. The finite life-time of the levels implies that they acquire a finite width, of the order of $\hbar\Gamma_j$; the energy of the level can then be represented by $E_j + i\hbar\Gamma_j/2$. A non perturbative quantum approach exists to compute these photon-molecule interaction amplitudes (e.g. Weisskopf & Wigner 1930). The amplitude of absorption and scattering has then a pole in $(\omega - \omega_{0j} - i\Gamma_j/2)^{-1}$. This introduces an imaginary part, that corresponds to absorption. We consider only the molecule in its ground state, absorbing a photon to reach the level j . To find the cross section, we must first sum all amplitudes:

$$\Psi \propto \sum_j \frac{\langle j|H|0\rangle e^{-i\omega_{0j}\tau}}{\omega - \omega_{0j} + i\frac{\Gamma_j}{2}}, \quad (\text{A1})$$

where $\langle j|H|0\rangle$ is the matrix element of the interaction, which can be considered here dipolar ($H = -\mathbf{d}\cdot\mathbf{E}$), since the photon wavelengths are assumed large with respect to the sizes of the molecules. The probability of transition from the initial to final state is the product of the above amplitude by the density of state, since a discrete level is coupled with a continuum of states (the photon energy is continuous). The density of states is $\rho(E) \propto E^2$, which introduces a term $\propto \omega^2$ as a function of photon frequency ω (cf. Cohen-Tannoudji et al. 1988). Since the square of the matrix element $\langle j|H|0\rangle$ is proportional to the square of the dipole, and also to ω , the total cross-section is proportional to ω^3 ; this dependency is retrieved in the spontaneous emission coefficient (A_{jk} , and the related Γ_j); although very close to the resonance, these coefficients are taken as constants, their ω dependency should be taken back to find the true shape of emission lines, slightly different from the Lorentzian shape (Arnous & Heitler 1953). It can be shown that in the vicinity of an electronic dipolar transition, between levels j and k , the line profile has the shape:

$$\sigma(\omega) = \frac{g_j \lambda_{jk}^2}{g_k} \frac{\left(\frac{\omega}{\omega_{jk}}\right)^3 \left(\frac{\Gamma_j}{2}\right)^2}{2\pi (\omega - \omega_{jk})^2 + \left(\frac{\Gamma_j}{2}\right)^2} \quad (\text{A2})$$

where the resonance occurs for $\omega = \omega_{jk}$ (with corresponding wavelength λ_{jk}), g_j and g_k are the statistical weights of the transition levels, and Γ_j is the natural width of the line (cf. Power & Zienau 1959). The numerator of this expression can be considered as a constant close enough to the resonance, and the classical Lorentzian profile is retrieved.

According to the optical theorem, the imaginary part of the forward scattering amplitude determines the total cross section for all processes, elastic and inelastic, for a given initial state of the photon (cf. for instance Landau

& Lifchitz 1989). We can consider the absorption cross-section from a stable fundamental state as equal to the total cross section of all possible scattering processes, since in absorbing a quantum, the molecule comes back to its fundamental state after emission of one or several photons.

Therefore the total absorption cross-section from the fundamental state, and in the vicinity of resonances, can be written as (cf. Landau & Lifchitz 1989):

$$\sigma(\omega) = \frac{\omega}{\epsilon_0 c \hbar} \sum_j |d_{0j}|^2 \frac{\left(\frac{\omega}{\omega_{0j}}\right)^3 \frac{\Gamma_j}{2}}{(\omega - \omega_{0j})^2 + \left(\frac{\Gamma_j}{2}\right)^2} \quad (\text{A3})$$

i.e. the shape of the diffused line coincides with the natural shape of the spontaneously emitted line.

It is convenient to introduce the dimensionless oscillator strengths $f_{0j} = \frac{2m_e}{\hbar e^2} \omega_{0j} |d_{0j}|^2$, where m_e is the electron mass and $|d_{0j}|$ is the matrix element of the dipole (and $g_j f_{jk} = g_k f_{kj}$). The width of each level is computed by summing the probabilities of spontaneous desexcitation to every lower levels: $\Gamma_j = \sum_k A_{jk}$, and the spontaneous rates are expressed by:

$$A_{jk} = \frac{2r_0}{3c} f_{jk} \omega_{jk}^2, \quad (\text{A4})$$

where $r_0 = e^2 / (4\pi\epsilon_0 m_e c^2)$ is the classical electron radius. The total cross section can then be expressed in terms of the Thomson section $\sigma_T = \frac{8\pi}{3} r_0^2$:

$$\begin{aligned} \sigma(\omega) &= \frac{3\sigma_T c}{4r_0} \sum_j \frac{\omega^4}{\omega_{0j}^4} f_{0j} \frac{\frac{\Gamma_j}{2}}{(\omega - \omega_{0j})^2 + \left(\frac{\Gamma_j}{2}\right)^2} \\ &= \frac{\sigma_T}{4} \sum_j \frac{\omega^4}{\omega_{0j}^4} f_{0j} \frac{\sum_k f_{jk} \omega_{jk}^2}{(\omega - \omega_{0j})^2 + \left(\frac{\Gamma_j}{2}\right)^2} \end{aligned} \quad (\text{A5})$$

Although there does not exist a simple analytical formula valid over the whole frequency range, the cross section is defined through approximations in the three domains of non-resonant, resonant and free (high frequencies). At the low frequency limit $\omega \ll \omega_{0j}$, the photon-molecule interaction reduces to the Rayleigh diffusion $\propto \omega^4$:

$$\sigma(\omega) = \sigma_T \omega^4 \left[\sum_j \frac{f_{j0}}{(\omega_{0j}^2 - \omega^2)} \right]^2, \quad (\text{A6})$$

and at high energy, the cross section reduces to that of free electrons, σ_T , since the electron binding energy is then negligible. At high energy the cross section is anyway not realistic since the formulae for the ground state ignore ionization and other high-energy effects.

For the summation we consider all Lyman and Werner lines, as tabulated in Abgrall & Roueff (1989). Since we are concerned only with H₂ molecules initially in their ground state ($J = 0, v = 0$), we have considered only

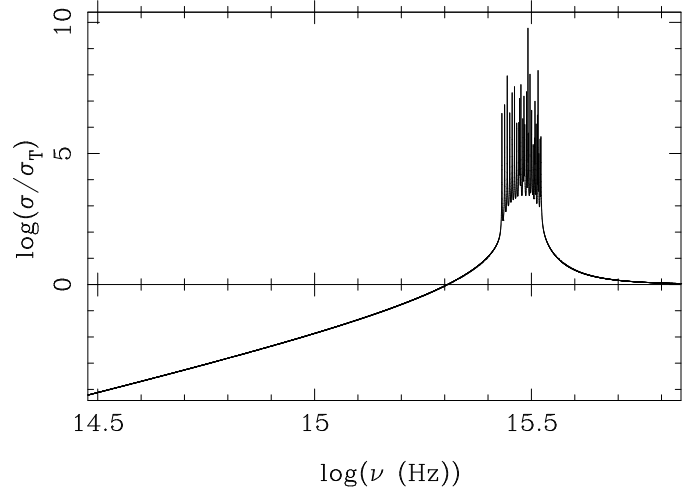


Fig. 5. Computation of the cross section corresponding to the interaction of photons with H₂ molecules in their ground state, normalised to the Thomson cross section $\sigma_T = 6.652 \cdot 10^{-25} \text{ cm}^2$.

$R(0)$ transitions (where $\Delta J = 1$) and tabulated 21 and 7 levels respectively in the Lyman and Werner bands. The shape of the total cross section is plotted as a function of frequency in Fig. 5.